Asian Journal of Chemistry; Vol. 24, No. 12 (2012), 5525-5529

ASIAN JOURNAL OF CHEMISTRY

www.asianjournalofchemistry.co.in

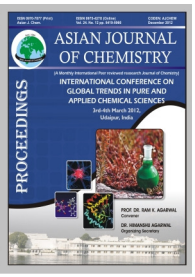

Preparation and Characterization of Pt Based Mono and Bimetallic Nano Catalysis and Their Application of Citral Hydrogenation†

S.A. Ananthan*, V. Narayanan, R. Suresh and K. Giribabu

Department of Inorganic Chemistry, School of Chemical Sciences, University of Madras, Guindy Campus, Chennai-600 025, India

*Corresponding author: E-mail: saananth2@yahoo.com

AJC-11685

Carbon nanotubes supported Pt, Ru and Pt-Ru catalysts were prepared by impregnation method and reduced at two different temperatures, 375 ºC (LTR) and 675°C (HTR). The catalysts were characterized by BET surface area measurement, TPD, HR-SEM, EDAX, HR-TEM, XRD and XPS. It was found that the XRD of Pt showed fcc crystalline structure and Ru showed hcp crystalline structures, which is uniformly dispersed with an average particles size of 3.5 nm and zero valence metallic state. The removal of acidic oxygen surface group is observed when heat-treatments in an inert atmosphere at 675 ºC were performed. The bimetallic catalyst of Pt-Ru/MWCNT was found to afford remarkably high conversion levels (88 %) and high selectivity (90 %) provided that a thermal pre-treatment was performed on the catalyst. These results can be rationalized in terms of electron transfer from the support to the metal. The catalysts are environment friendly and can be recycled for more than eight times.

Key Words: Citral hydrogenation, Pt-Ru bimetallic catalysts, Multi-walled carbon nanotube supported catalyst, HR-TEM, XRD, XPS.

INTRODUCTION

Selective hydrogenation of α, β-unsaturated aldehydes to their corresponding alcohols is a process of major interest for the chemical industries, especially the fine chemical industries, such as for the production of pharmaceuticals, cosmetics, detergents, flavours and fragrances[1-3]. Many studies on hydrogenation of crotonaldehyde, cinnamaldehyde and citral over transition metal catalysts were reported in the literature and Pt has been proved to be one of the most effective components in these reactions[4,5]. Among all these compounds, citral (3,7-dimethyl-2,6-octadienal) belongs to this class of organic compounds and has three unsaturated bonds a conjugated system comprized of C=C and C=O groups as well as an isolated C=C bond. In particular, citronellal is formed by hydrogenation of the olefinic bond which is conjugated to the C=O group whereas hydrogenation of the simultaneously yields the unsaturated allyl-group alcohols in the trans and *cis* forms geraniol and nerol, respectively. Under certain reaction conditions and depending on the catalyst type, consecutive hydrogenation reactions can occur leading various products to geraniol, nerol, citronellal, citronellol, dihydrocitro-nellal, iospuecol and 3,7-dimethyloctanol. Liquid phase selective hydrogenation of C=O group can often be controlled by the nature of the individual metal, the presence of a second metal (bimetallic catalysts), metal particle size (dispersion), thermal treatment by the catalyst support material, steric constraints in the metal environment and strong metal-support interactions (SMSI). The influence of the above discussed parameters on activity and selectivity of catalysts for the selective hydrogenation of α, β-unsaturated aldehydes has been reviewed[6] and can also be found in numerous studies of citral hydrogenation over supported metal catalysts in the past years[7-14]. However, carbon materials are widely chosen as supports for hydrogenation of catalysts, various carbon materials have been used in different reaction such as active carbons[15], carbon fibers[16,17], carbon cloth[18] active felt[19] and carbon nanotubes[20]. The novel CNT structures were found to have remarkable catalytic effect when used as support for selective hydrogenation reaction[21,22]. In fact multi-walled carbon nanotubes (MWCNTs) supported Pt catalysts have been successfully used to selective hydrogenation of citral and got a desirable compound[23]. Among other factors, the electronic effects of the support, the presence of a second metal and the metal particle sizes and morphology, could enhance selectivity. Considering the better selectivity presented by Pt and Ru catalysts, these metals were used as active phases. In this work, we report the preparation of Pt, Ru and Pt-Ru multi-walled supported catalysts by the impregnation method, being reduced in two different temperatures, 375 ºC and 675 ºC. The catalysts are characterized by BET

†Presented at International Conference on Global Trends in Pure and Applied Chemical Sciences, 3-4 March, 2012; Udaipur, India

surface area, TPD, XRD, HRSEM with EDXA, HRSEM and XPS techniques and their catalytic activity for selective hydrogenation of citral towards unsaturated alcohols (geraniol and nerol) under mild conditions on high temperature treated catalysts supported on MWCNT.

EXPERIMENTAL

Muiltwalled carbon nanotube (99.9 % from Sigma-Aldrich) supported Pt, Pt-Ru nanocatalysts prepared by impregnation methods. To deposit Pt/or Ru precursors onto functionalized MWCNT, 0.1 g of MWCNT was immersed in $H_2PtCl_6 \cdot 6H_2O$ (99.9 % Alfa-Aesar)/or $RuCl_3 \cdot 6H_2O$ (99 % Alfa-Aesar) aqueous solution with 40 mL of ethylene glycol (99.8 % Sigma-Aldrich). $NaBH_4$ was added drop by drop, to the mixtures with vigorous stirring for the complete reduction of Pt/or Ru form their respective metal salts. After that 10 min of ultrsonication, the reaction was performed at 165 ºC with magnetic stirring for 30 min. The catalysts were separated from ethylene glycol and washed with deionized water, followed by drying at 200 ºC in vacuum. The as prepared catalyst was noted at Pt/MWCNT or Ru/MWCNT and the pre-treatment at 300 ºC, expected loading is 5 % and confirmed by inductively coupled plasma (ICP) measurements. The prepared catalysts were heat treatment at two different temperatures, at 375 and 675 ºC in a nitrogen flow (20 mL/min) for 2 h to remove the oxygen-containing groups from MWCNT surface. The resulting catalysts were denoted as Pt/MWCNT375, Pt/MWCNT675, Ru/MWCNT375 and Ru/MWCNT675. The preparations of bimetallic catalysts were similar to that of Pt/MWCNT in the presence of both Pt and Ru metal precursor salts. The Pt-Ru loading was kept at 5 wt % and the molar ratio of Pt to Ru was 1:1. The prepared catalyst denoted as Pt-Ru/MWCNT and followed by pre-heated at two difference temperatures and denoted as Pt-Ru/MWCNT375, Pt-Ru/ MWCNT675. The elemental compositions were measured by ICP analysis and the results are shown in Table-1.

TABLE-1
SAMPLE CODES, LOADINGS AND PRE-TREATMENT CONDITIONS OF THE VARIOUS MWCNT SUPPORTED Pt, Ru AND Pt-Ru CATALYSTS

Catalysts	Loading (%)		Gas-phase pre-reduction (ºC)	Heat treatment in N_2 (ºC)
	Pt	Ru		
Pt/MWCNT	5.0	0.0	300	0
Ru/MWCNT	0.0	5.0	300	0
Pt-Ru/MWCNT	2.5	2.5	300	0
Pt/MWCNT375	4.5	0.0	300	375
Pt/MWCNT675	4.7	0.0	300	675
Ru/MWCNT375	0.0	4.8	300	375
Ru/MWCNT675	0.0	5.1	300	675
Pt-Ru/MWCNT375	2.4	2.6	300	375
Pt-Ru/MWCNT675	2.2	2.8	300	675

Catalyst characterization: TPD was conducted to determine the amounts of surface oxygen functional group of supports at 375 and 675 ºC under helium on micrometrics autochem 2910. The decomposition products (CO and CO_2) of the complexes were analyzed by mass spectrometry. The BET surface area measurements were made on a micromeritics Gemini 2360 instrument by N_2 adsorption at liquid nitrogen temperature. Prior to measurements, samples were oven dried at 120 ºC for 12 h and flushed with argon gas for 2 h. SEM analysis was carried out with a Jeol JSM 5410 microscope, operating with an accelerating voltage of 15 kV. Micrographs were taken after coating by gold sputtering. Elemental analysis was carried out on a Kevex, Sigma KS3 energy dispersive X-ray instrument operating at a detector resolution of 136 eV. TEM photographs were taken with a Hitachi H-7500 electron microscope at an accelerating voltage of 80 kV. The crystalline structure and elemental analysis of the nanoparticles were characterized by a JEOL JEM-2010 field emission high-resolution electron transmission microscopy (HRTEM) equipped with EDS at an accelerating voltage of 200 kV. X-ray diffraction techniques are based on the elastic scattering of X-rays from structures that have long order. The diffraction pattern generated is used to study surface-supported nanoparticles, affording information on the crystal phase, lattice constant and average particle size of nanoparticles. XPS technique provides a compositional estimate of only the outermost layers, with a penetration depth of *ca.* 5-15 nm. The spectral regions of the Pt 4*f*, Ru 3*d* and O1*s*, C1*s*, peaks were acquired. In charge-up correction, the calibration of binding energy (BE) of the spectra was referenced to the C1s electron bond energy corresponding to graphitic carbon at 284.5 eV. The samples were also analyzed by infrared spectroscopy on Perkin-Elmer 2000 FT-IR spectrometer.

Citral (mixture of E and Z forms, Merck, 99 %) and isopropanol (Fluka, 99.5 %) are used as received. The liquid phase citral hydrogenation experiments were performed in a stirred semi-batch reactor. Before the reaction the catalysts were reduced in situ under hydrogen (gas purity, 99.995 %) flow (80-100 mL/min) for 2 h under 10 MPa at 250 ºC. Then, the reactor was cooled to reaction temperature. Reactant mixture (200 mL of 0.1 M citral in isopropanol) was injected into the bubbling unit to remove the dissolved oxygen before it was injected into the reactor and contacted with the catalysts. Citral hydrogenation reaction was performed at 90 ºC, 10 MPa and at a stirring speed of 750 rpm which are previously studied.

RESULTS AND DISCUSSION

Catalysts surface morphology and structure characterization in Table-2 shows the result of BET surface area of the synthesized samples of mono and bimetallic catalysts are reduced at two temperatures, 375 and 675 ºC. It is observed that the synthesized support has a high surface area of Pt-Ru/MWCNT675 catalyst is 380 m^2g^{-1}, while Pt/MWCNT catalyst has shown a specific surface area of 242 m^2g^{-1}. Surface area is one of the important features that highly influence the catalyst activity. Large surface area, results in more available reaction sites for adsorption of reactive components and hence higher activity. As it can be seen from the Table-2 that the increasing of temperature and loading of Pt on MWCNT does not greatly change the specific surface area of the catalysts.

TPD is a method of charaterization of adsorbed surface species by heating sample and simultaneously, detecting the residual gas by means mass spectrometry. As the temperatyure rises, certain adsorbed species will have enough energy to escape from the surface. The temperature at which the species

TABLE-2
STRUCTURAL PARAMETERS AND COMPOSITIONS OF Pt, Ru AND Pt-Ru CATALYSTS REDUCED AT 375 ºC AND 675 ºC

Catalysts	BET (m^2/g)	2θ			BE (eV)			Particle size (nm)
		C(002)	Ru(101)	Pt(111)	O 1*s* /C 1*s*	Ru3$d_{5/2}$	Pt4$f_{7/2}$	
Pt/MWCNT	242	26.3	0	39.5	531.21 (284.52)	0	70.05	3.2
Ru/MWCNT	238	26.4	43.7	0	531.02 (284.14)	280.15	0	3.2
Pt-Ru/MWCNT	225	26.6	43.8	39.6	531.82 (284.76)	280.21	70.13	3.5
Pt/MWCNT375	250	26.6	0	39.5	531.28 (284.51)	0	70.10	3.5
Pt/MWCNT675	280	26.7	0	39.5	531.50 (284.45)	0	70.21	3.8
Ru/MWCNT375	240	26.5	43.8	0	531.42 (284.72)	280.23	0	3.3
Ru/MWCNT675	285	26.6	43.9	0	531.29 (284.57)	280.33	0	3.6
Pt-Ru/MWCNT375	320	26.7	43.7	39.5	531.81 (284.71)	280.35	70.23	3.8
Pt-Ru/MWCNT675	380	26.7	43.8	39.7	531.82 (284.75)	280.43	70.38	4.2

are relased provides information about their binding energy to the surface. Analyzing the amount of CO and CO_2 released during the TPD experiments it can be observed that part of the surface group are removed during the catalyst prepartion. Thus, the amount of CO_2 evolved during the TPD expereincements changes from 950 to 468 μmol g^{-1}, corresponding to a decrease of 50 % in the concentration of these sites. This can be attributed to the disppearance of caboxylic acid group. These group are activity involved the anchoring of the Pt precursor, allowing high dispersion and loadings. It has been recently edidenced that finely dispersed Pt clusters to the MWCNT surface *via* bonding with the ionic form of carboxylate-COO(Pt)[24]. The powder X-ray diffraction patterns of Pt-Ru/MWCNT catalysts are shown in Table-1. The first peak at 26.4º is attributed to the graphite (002) plate of the MWCNTs support. The other four peaks are characteristic of face centered cubic (fcc) crystalline, corresponding to the planes (111), (200), (220) and (311) at 2θ values of 39.6, 46.8, 67.3 and 81.2º respectively. It is important to note that the diffraction peaks indicating the presence of either pure Ru or Ru-rich hexagonal close packed (hcp) phase is appear to the plan (101), which suggests that Ru atoms either from an alloy with pt or exist as oxides in an amphorphose phases. It can be displayed that the diffraction peaks for the Pt-Ru catalysts are evidently shifted to the higher 2θ values. Its difference that the diffraction peaks are shifted in the XRD patterns, results in different alloying degree. Because Ru atomic radius is smaller than that of Pt atom, following on Vegard's law, the lattice parameters of Pt-Ru/MWCNT catalysts decrease when Ru atoms incorporate into the fcc structure of Pt. The lattice parameters and d values of the Pt, Ru and Pt-Ru catalysts are given in Table-2. XPS was study the compositions and electronic states of WMCNT supported nanoparticles. Fig. 1a show survey spectra of Pt-Ru/MWCNT in the survey spectra, there are peaks of Pt 4*f*; Ru 5*d*, C 1*s* and O 1*s* are common in all the carbon supported catalysts. Fig. 1b show the XPS of Pt 4*f* spectrum for the Pt-Ru/MWCNT catalyst reduced at two different temperatures. The Pt 4*f* spectrum shows a doublet containing a low energy band (Pt 4$f_{7/2}$) and a high energy band (Pt 4$f_{5/2}$) at 71.2 and 74.6 eV, respectively. These binding energy values are in good agreement with the literature data for Pt (Hufner and Wertheim, 1975). These peaks indicated that Pt is present in metallic state, Pt (0). The Table-2 shows, the Ru 3*d* spectrum has Ru 3$d_{5/2}$ and Ru 3$d_{3/2}$ at 280.2 and 284.1 eV, their peaks indicate that Ru is present in metallic state Ru (0).

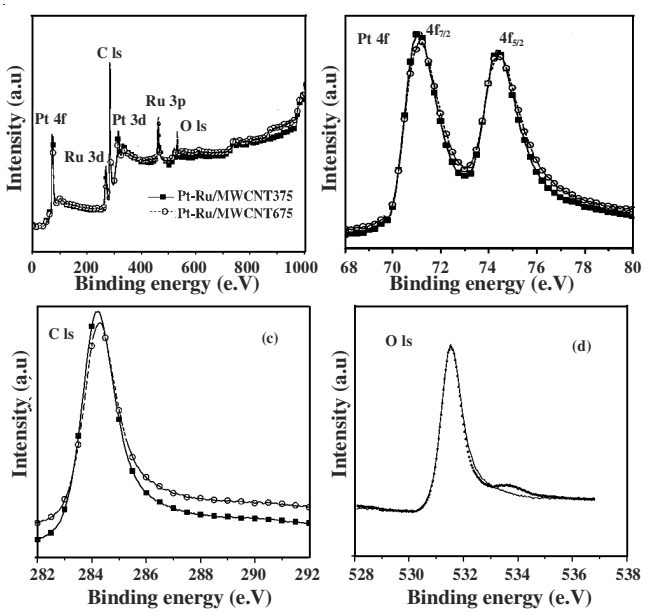

Fig. 1. XPS spectra of (a) Pt-Ru/MWCNT catalysts; (b) Pt 4*f* core level; (c) C 1s core level; (d) O 1s core level

The chemical changes of mono and bimetallic MWCNT supported samples due to reduced at different temperatures. Fig. 1c shows, the peak at 284.3 eV, observed in all spectra, is generated by photoelectrons emitted from the C 1s core level while the structure peaking near 530 eV in the spectrum recorded on MWCNT sample is due to emission from the O 1s core level shows in Fig. 1d. Note that the relative intensity of the C 1s line in the XPS spectrum is reduced by the presence of Pt nanoparticles at the MWCNT surface. Due to inelastic scattering some electrons emitted from carbon atoms localized below the Pt clusters will lose part of their kinetic energy when passing through them, no longer contributing to the C 1s peak. The micrographs of Fig. 2 show the HRSEM and their corresponding EDXA images were shown. The presence of Pt and Ru metal nanoparticle in the modified by thermal treated catalysts were confirmed by EDX analysis. From Fig. 2, it was observed that nonoparticles with less than 3.5 nn are deposited on the surface of multiwall carbon nanotubes. TEM images we observe the deposits of mono and bimetallic catalysts on the MWCNT support naonoparticles. The nanoparticles are in smaller size and good dispersion on the support. For Pt-Ru/WMCNT675, the presence of large amount of agglomeration is observed and some of the carbon nanotube particles were not covered by Pt-Ru/MWCNT nanoparticles.

The histograms for particle size distribution are shown in Fig. 3. The average particle sizes were 3.3, 3.2, 3.5 for Pt/MWCNT675, Pt-Ru/MWCNT375, Pt-Ru/MWCNT675; respectively. The FT-IR spectra of MWCNTs are plotted in Fig. 4, the assignment of the main bands observed to the functional groups. A peak at 2922 cm^{-1} can be assigned to the C-H_n functional groups or to the C-H stretching mode of the functionalized alkyl chains in the MWCNTs[25]. A broad band at 3435 cm^{-1} is assigned to a variety of O-H stretching modes. The wide width of this band suggests that several different-OH groups are probably present in many different chemical environments[26]. Carboxylic acid groups are likely indicated by the C=O stretching band at 1633 cm^{-1}. The band at 1162 cm^{-1} is located in the range of C-OH stretching modes of ethers, esters, alcohols and phenol compounds. The band at 1466 cm^{-1} is assigned conjugation of C=C bond interaction between localized. Intensity of the peak indicates changes of the dipole moment that is bigger with increasing polarity of the group[27]. In general, the FT-IR spectra suggest that the surface of the MWCNTs is prone to absorb many hydroxyl and carbonyl groups. From a comparison of the plots of the LTR and HTR samples, it seems that in the former, many polar groups are generated on the nanotubes than after the thermal treatment.

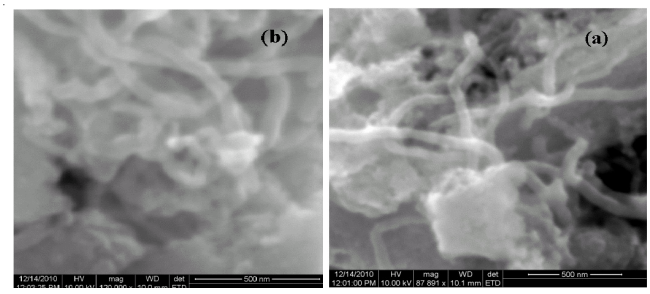

Fig. 2. SEM micrographs of Pt-Ru/MWCNT catalyst reduced at (a) 375 ºC and (b) 675 ºC under nitrogen

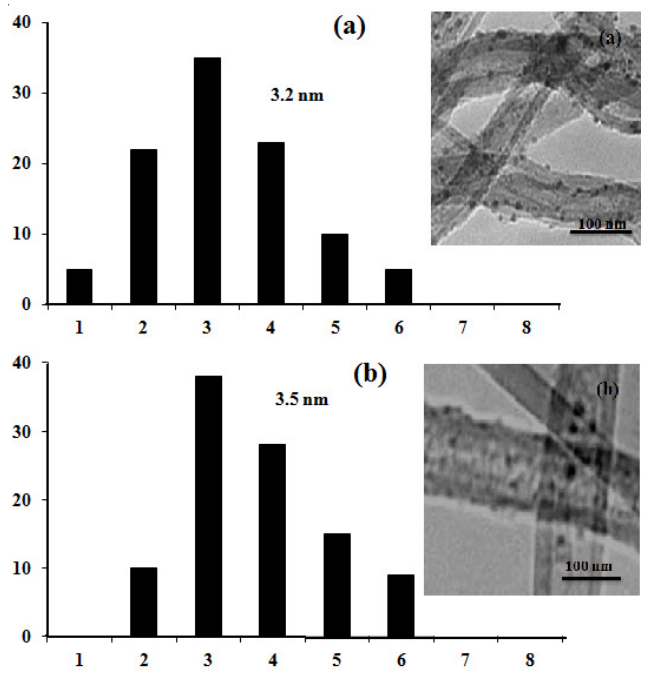

Fig. 3. HRTEM with histograms for particle size distributions of Pt-Ru/MWCNT catalyst reduced at (a) 375 ºC and (b) 675 ºC under nitrogen

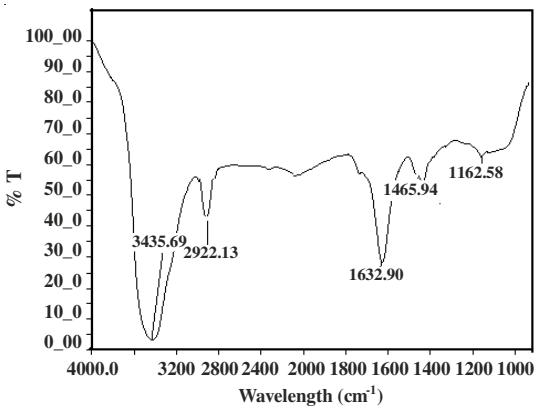

Fig. 4. FT-IR spectra of treated Pt-Ru/MWCNT375

Effects of Ruthenium promoter on Pt catalysts, which that the formation of these heterogeneous bimetallic compounds could explain the greater activity and selectivity observed with the Pt-Ru/MWCNT samples with respect to the monometallic Pt/MWCNT and Ru/MWCNT ones. Based on the TPD and XPS results, it is assumed that on the surface of Pt-Ru/MWCNT catalysts there are clusters formed by both Pt^0 and Ru^0 atoms in intimate contact. This contact between both types of atoms favours the electronic transfer from Ru^0 towards Pt^0, as determined by XPS. In this way, there is δ^+ charge density in the Ru atoms and a δ^- charge density in the Pt atoms (**Scheme-I**). On the other hand, considering a molecule of α, β-unsaturatedaldehyde, it is accepted that the functional C=O group could be adsorbed on top, di-σ_{co} and π_{co} over a metal surface. Similarly, for the C=C group, the most likely adsorption modes are di-σ_{cc} and π_{cc}. According to the analysis performed by Delbecq and Saute[28], taking into account the interaction of different α,β-unsaturatedaldehydes with Pt, as an average, the bonding energy follows the order; di-σ_{co}= π_{co} > on-top. On the other hand, the bonding energies calculated for di-σ_{cc} and π_{cc} are comparable to those of di-σ_{co} and π_{co}. Based on this analysis, it is expected that, in the citral hydrogenation, gernol/nerol and citronellal would be obtained in similar amounts over Pt^0 clusters. Results reported by other authors for the citral hydrogenation in liquid phase with Pt-based catalysts are in agreement with this analysis[29]. However, on a bimetallic Pt-Ru surface, it is likely that the following interactions are the most favoured; (a) on-top adsorption over $Ru^{\delta+}$ (**Scheme-Ia**); di-σ_{co} adsorption over $Pt^{\delta-}$-$Ru^{\delta+}$ (**Scheme-Ib**); π_{co} adsorption over $Pt^{\delta-}$ (**Scheme-Ic**). The on-top adsorption over $Ru^{\delta+}$ is more probable than over Pt^0 of monometallic Pt/MWCNT catalyst. This is due to the fact that the electrophilic character of Ru in the bimetallic Pt-Ru compound is much higher than that of Pt^0 in monometallic Pt/MWCNT. As a consequence, the interaction of an electron pair of the oxygen in the C=O group with a $Ru^{\delta+}$ sites is much more likely than with Pt^0. The di-σ_{co} adsorption would occur by the interation between the O atom and $Ru^{\delta-}$ and between the C atom and $Pt^{\delta-}$ (**Scheme-Ib**). The $C^{\delta+}$-$O^{\delta-}$ charge separation, enhanced after the interaction with the actives site, is favouring the di-σ_{co} adsorption over a $Pt^{\delta-}$ $Ru^{\delta+}$ site against a Pt-Pt site. Likewise, the π_{co} adsorption over $Pt^{\delta-}$ would be favoured with respect to Pt^0. This may be explained by the back bonding from the platinum orbital with increased electronic density in the bimetallic samples towards

the π* molecular orbital of C=O group. This would further weaken the C=O bond adsorbed in π_{co} mode activating it for its subsequent hydrogenation to C-OH. In all cases, the hydrogen dissociatively adsorbed in neighboring Pt atoms would allow the easy hydrogenation of the functional C=O group adsorbed in one of the proposed modes (**Scheme-I**), all of which are more active than the C=O group adsorbed on a Pt^0 cluster. When the citral is adsorbed through the C=O group over the bimetallic Pt-Ru surface, the interaction with the C=C bond would be decreased by the repulsion effect between the citral substituting group and Pt-Ru surface (**Scheme-I**). The ratio of the repulsion forces with respect to the attraction forces, between the citral substituting group and the metallic surface, is increasing by the higher electronic density of Pt orbitals in the bimetallic samples with respect to monometallic Pt/MWCNT; the extension of the *d* orbitals of Ru. However, the interaction between the C=C bond and the Pt atoms is still possible through the π_{cc} adsorption mode. This adsorption mode, similar to what occurs with the π_{co} mode, would be favoured over $Pt^{\delta-}$ with respect to Pt^0, explaining the higher hydrogenation rate of citral to citranallal over Pt-Ru/MWCNT than over Pt/MWCNT and Ru/MWCNT catalysts. However, on the basis of the results obtained in this work, the increase in the activation of conjugated C=C bond is less important than the activation increase of the C=O group by adsorption through modes on- top, di-σ_{co} and π_{co} over Pt-Ru catalysts.

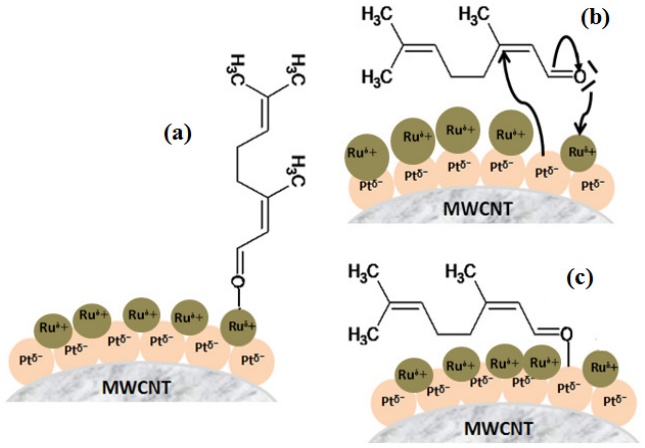

Scheme-I: Citral adsorption modes over Pt-Ru/MWCNT catalysts: (a) on-top; (b) di-σ_{co}; (c) π_{co}

The probability of interaction of these activation of the functional C=O group and, to a lesser extent, of the C=C bond with the catalytic surface is expected to be higher with the bimetallic Pt-Ru/MWCNT catalysts than with monometallic of Pt/MWCNT and Ru/MWCNT catalysts. This would explain the higher activity of the former in the citral hydrogenation in liquid phase. On the other hand, the higher probability of interation and activation of the functional C=O group with respect to the C=C bond would also explain the high selectivity towards unsaturated alcohols (geraniol and nerol) observed with these bimetallic catalysts.

Conclusion

The selectivity towards unsaturated alcohols (geraniol and nerol), the results highly depended on the surface properties of the MWCNT support and promoter. Removal of oxygen-containing group from MWCNT surfaces elevated both activity and selectivity, due to the suppressed side reactions catalyzed by acid and enhanced electron transfer from MWCNT to Pt nanoparticles. The close contact between Pt and promoter (Ru) nanoparticles, which attains the affinity between MWCNT and citral due to the π-π interaction and assists the metal metal electron transfer. These synergic effects contributed to the significantly improved activity and high selectivity. The use of a Pt-Ru/MWCNT675 system leads to higher selectivity than that obtained with monometallic systems. However, we have demonstrated that MWCNT supported bimetallic catalysts, high temperature reduction, which increases the particle size of the metal, significantly promotes the selectivity unsaturated alcohols, probably due to an electron transfer route from the MWCNT to the metal.

ACKNOWLEDGEMENTS

The authors thank to National Centre for Nanoscience and Nanotechnology (NCNSNT), University of Madras for recording FE-SEM, HR-TEM and EDAX and also thank to IIT Madras for recoding XPS.

REFERENCES

1. V. Ponec, *Appl. Catal. A,* **149**, 27 (1997).
2. P. Claus, *Top. Catal*., **5**, 51 (1998).
3. P. Gallezot and D. Richard, *Catal. Rev. Sci. Eng*., **40**, 81 (1998).
4. M.A. Aramendia, V. Borau, C. Jimenez, J.M. Marinas, J.R. Ruiz and F.J. Urbano, *J. Mol. Catal. A*, **171**, 153 (2001).
5. U.K. Singh and M.A. Vannice, *J. Catal*., **191**, 165 (2000).
6. P. Maki-Arvela, J. Hajek, T. Salmi and D. Murzin, *Appl. Catal. A*, **292**, 1 (2005).
7. D. Manikandan, D. Divakar and T. Sivakumar, *Catal. Lett.*, **123**, 107 (2008).
8. U.K. Singh and M.A. Vannice, *J. Mol. Catal. A: Chem*., **163**, 233 (2000).
9. C. Milone, R. Ingoglia and S. Galvagno, *Gold Bull.*, **39**, 54 (2006).
10. S. Mukherjee and M.A. Vannice, *J. Catal*., **243**, 108 (2006).
11. U.K. Singh, M.N. Sysak and M.A. Vannice, *J. Catal*., **191**, 181 (2000).
12. U.K. Singh and M.A. Vannice, *J. Catal*., **191**, 165 (2000).
13. A.M. Silva, O.A.A. Santos, M.J. Mendes, E. Jordao and M.A. Fraga, *Appl. Catal. A*, **241**, 155 (2003).
14. S. Mukherjee and M.A. Vannice, *J. Catal*., **243**, 131 (2006).
15. J.C. Serrano-Ruiz, A. Sepulveda-Escribano, F. Rodriguez-Reinoso and D. Duprez, *J. Mol. Catal. A. Chem*., **268**, 227 (2007).
16. J. Aumo, S. Oksanen, J.P. Mikkola, T. Salmi and D.Y. Murzin, *Catal. Today,* **102**, 128 (2005).
17. I.M.J. Vilella, S.R. de Miguel, C.S.M. de Lecea, A. Linares-Solano and O.A. Scelza, *Appl. Catal. A. Gen*., **281**, 247 (2005).
18. J. Aumo, S. Oksanen, J.P. Mikkola, T. Salmi and D.Y. Murzin, *Ind. Eng. Chem. Res*., **44**, 5285 (2005).
19. I.M.J. Vilella, S.R. de Miguel and O.A. Scelza, *Latin Am. Appl. Res*., **35**, 51 (2005).
20. E. Asedegbega-Nieto, A. Guerrero-Ruiz and I. Rodriguez-Ramos, *Carbon*, **44**, 804 (2006).
21. H.X. Ma, L.C. Wang, L.Y. Chen, C. Dong, W.C. Yu, T. Huang and Y.T. Qian, *Catal. Commun.*, **8**, 452 (2007).
22. Y. Li, G.H. Lai and R.X. Zhou, *Appl. Surf. Sci*., **253**, 4978 (2007).
23. F. Qin, W. Shen, C.C. Wang and H.L. Xu, *Catal. Commun*., **9**, 2095 (2008).
24. R.V. Hull, L. Li, Y.C. Xing and C.C. Chusuei, *Chem. Mater.*, **18**, 1780 (2006).
25. W.Z. Li, C.H. Liang, W.J. Zhou, J.S. Qiu and Z.H. Zhou, *J. Phys. Chem. B*, **107**, 629 (2003).
26. Y.Q. Liu and L.A. Gao, *Carbon,* **43**, 47 (2005).
27. C. Jie and S. Qize, PR Beijing, p. 48. (1996).
28. F. Delbecq and P. Sautet, *J. Catal*., **164**, 152 (1996).
29. A.F. Trasarti, A.J. Marchi and C.R. Apesteguia, *J. Catal.*, **247**, 155 (2007).